ARTICLE
Journal of Cellular Biochemistry 113:2086–2097 (2012)

Journal of Cellular Biochemistry

Inhibition of IGF-IR Increases Chemosensitivity in Human Colorectal Cancer Cells Through MRP-2 Promoter Suppression

Ke Shen,[1] Daling Cui,[1] Liyun Sun,[1] Yanhua Lu,[1] Mingquan Han,[2*] and Jianwen Liu[1**]

[1] *State Key Laboratory of Bioreactor Engineering and Shanghai Key Laboratory of Chemical Biology, School of Pharmacy, East China University of Science and Technology, #268, 130 Meilong Road, Shanghai 200237, P.R. China*

[2] *Shanghai Pulmonary Hospital, Tongji University School of Medicine, Shanghai, 200433, P.R. China*

ABSTRACT

The emergence of multidrug resistance (MDR) in cancer cells has made many of the currently available chemotherapeutic agents ineffective. However, the mechanism involved in mediating this effect is not yet fully understood. Here, we found the overexpression of type I insulin-like growth factor receptor (IGF-IR) in established colorectal MDR cells. Specific siRNA of IGF-IR decreases cell proliferation, exert synergistic effect with anticancer drugs. The downstream signaling of IGF-IR, PI3K/AKT pathway, was altered upon IGF-IR silencing. The expression of multidrug-resistance-associated protein 2 (MRP-2) was suppressed due to the nuclear translocation of nuclear factor-like 2 (Nrf2). Then the intracellular drug concentration was increased and the drug-resistant phenotype was reversed. Our findings improve current understanding of the biology of IGF-IR and MDR and have significant therapeutic implications on colorectal MDR cancer. J. Cell. Biochem. 113: 2086–2097, 2012.

KEY WORDS: INSULIN-LIKE GROWTH FACTOR TYPE I; MULTIDRUG-RESISTANCE; COLORECTAL CANCER; RNA INTERFERENCE; MULTIDRUG RESISTANCE-ASSOCIATED PROTEIN 2

Colorectal cancer (CRC) is one of the most frequently occurring cancers worldwide. Significant improvements in patient survival rates have been achieved in recent years, largely due to the availability of targeted molecular therapies in addition to the standard chemotherapeutic regimens [Dallas et al., 2009]. However, the emergence of drug resistance has made many of the currently available chemotherapeutic agents ineffective. Many studies using tumor cell lines as model systems have demonstrated that exposure of cells to one drug often results in cross-resistance to many other structurally, chemically, and functionally distinct agents. This phenomenon is broadly known as the multidrug resistance (MDR) phenotype [Haimeur et al., 2004]. Overcoming MDR to conventional and targeted therapies remains a key challenge in fighting against cancer. One of the major mechanisms of MDR is the enhanced ability of tumor cells to actively efflux drugs leading to a decrease in cellular drug accumulation below toxic levels. Active drug efflux is mediated by several members of the ATP-binding cassette (ABC) superfamily of membrane transporters which have now been subdivided into seven families designated A through G [Haimeur et al., 2004]. These drug transporters are present in all tissues and cell types in different amounts and, in certain instances, on different membranes. Together, they are an important component of the defense mechanisms used both by normal and malignant cells against cytotoxic compounds. Among these members, MRP-2 is the most important biliary efflux pump known so far [Kauffmann et al., 2002]. MRP-2 is able to confer MDR in tumor cells, probably by

Abbreviations: IGF-IR, insulin-like growth factor type I receptor; MDR, multidrug resistance; CRC, colorectal cancer; LOHP, oxaliplatin; VCR: Vincristine; P-gp, P-glycoprotein; MRP, multidrug resistance-associated protein; siRNA, small RNA interference.

Additional supporting information may be found in the online version of this article.

Grant sponsor: Fundamental Research Funds for the Central Universities; Grant sponsor: Shanghai Leading Academic Discipline Project; Grant number: B507; Grant sponsor: 111 Project; Grant number: B07023.

*Correspondence to: Mingquan Han, Shanghai Pulmonary Hospital, Tongji University School of Medicine, Shanghai, 200433, P.R. China. E-mail: doctor_han@msn.com

**Correspondence to: Jianwen Liu, State Key Laboratory of Bioreactor Engineering and Shanghai Key Laboratory of Chemical Biology, School of Pharmacy, East China University of Science and Technology, #268, 130 Meilong Road, Shanghai 200237, P.R. China. E-mail: liujian@ecust.edu.cn

Manuscript Received: 26 October 2011; Manuscript Accepted: 19 January 2012

Accepted manuscript online in Wiley Online Library (wileyonlinelibrary.com): 24 January 2012

DOI 10.1002/jcb.24080 • © 2012 Wiley Periodicals, Inc.

eliminating drugs like Cisplatin or Vincristine in association with glutathione [Cui et al., 1999].

The insulin-like growth factor (IGF) signaling plays important roles in cell biology [Whittaker et al., 2010]. The IGF system is composed of the IGF ligands (IGF-I and IGF-II), receptors (IGF-IR and IGF-IIR), the insulin receptor (IR), and six regulatory IGF-binding proteins (IGFBPs). IGF-IR is activated via autophosphorylation after ligand binding, thereby leading to activation of the mitogenactivated protein kinase (MAPK) and phosphatidylinositol 3-kinase (PI3K) cascades [Garrouste et al., 2002]. Abundant data from cell culture, animal, and human epidemiological studies show that the insulin-like growth factors -I and -II and IGF-IR regulate growth, survival, metabolism, and metastasis of cancer cells [Thompson and Kakar, 2005; Chakraborty et al., 2010; Sachdev et al., 2010]. Aberrant expression of IGF-I, II, and IGF-IR is detected in many different types of cancer [Tanno et al., 2001; Natrajan et al., 2006; Tarn et al., 2008]. Although recent researches has been reported that IGF-IR inhibition can increases the drug sensitivity of tumor cells [Min et al., 2005; Dallas et al., 2008, 2009; Hopkins et al., 2010; Sachdev et al., 2010; Hart et al., 2011], little is known regarding the molecular mechanism behind it.

Nrf2 is ubiquitously expressed in many organs as a transcription factor by binding to antioxidant responsive element (ARE). Nrf2 levels are increased in some tumor tissues where over-expression may enhance drug resistance through transcription of antioxidant, xenobiotic metabolism, drug efflux pump, and intrinsic chemoresistance genes [Singh et al., 2006; Ohta et al., 2008]. It has been reported that mouse Mrp2, 3, 4, and 6 in liver are induced by several Nrf2 activators [Maher et al., 2008; Rushworth and MacEwan, 2011] while the mechanism in human cells is still unclear.

It is interested to clarify the relationship between IGF-IR and MDR phenotype. In this present study, an Oxaliplatin (LOHP; LOHP is the mainstay of chemotherapeutic regimens for metastatic CRC) resistant sub-cell-line of human CRC cell line HCT116 and a Vincristine (VCR; VCR is a Broad-spectrum anticancer drug) resistant sub-cell-line of human CRC cell line HCT8 were employed as our models. IGF-IR mRNA and protein levels were both found higher in MDR cells than in their parental lines. LOHP and VCR were reported as substrates for MRP-2, so we hypothesized that IGF-IR overexpression may involve in MRP-2 mediated MDR in CRC cells. To verify this hypothesis, IGF-IR-specific small interference RNA (siRNA) was performed to knock down IGF-IR mRNA. IGF-IR inhibition by siRNA could reduce cell growth, arrest cell cycle, induce multidrug-resistant CRC cells apoptosis in a significantly lower dose of anticancer drugs and cause a reduction in four kinds of anticancer drugs IC_{50}. We also showed that MRP-2 were down regulated by IGF-IR/AKT/Nrf2/ARE signaling blocking through promoter suppression and result in a reversal of drug-resistant phenotype eventually.

MATERIALS AND METHODS

REAGENTS

Antibody against β-actin, AKT, phosphor-AKT-Ser473, Nrf2, Lamin B, Bcl2, Bax, Cyclin B1, MRP-1, MRP-2 were all from Santa Cruz Biotechnology (Santa Cruz Biotechnology Inc., CA). Antibodies against IGF-IR and phospho-IGF-IR-Tyr1161 were from Bioworld (Bioworld Technology Co. Ltd., MN). P-gp antibody was from eBioscience (eBioscience Inc., CA). Dual luciferase reporter assay system was from Promega (Promega Corporation, WI). PGL3-Promoter, PGL3-Basic and PRL-TK vectors were purchased from Promega. pcDNA 3.1(+) was from Invitrogen (Invitrogen Corporation, CA). IGF-IR-specific inhibitor PPP and AKT-specific inhibitor SH-5 were from Merck (Merck & Co., Inc., Darmstadt, GER). All other chemicals were from Sigma–Aldrich unless otherwise stated.

CELL CULTURE AND MDR CELL LINE ESTABLISH

HCT8 human ileocecal colorectal adenocarcinoma cell line and HCT116 human colorectal carcinoma cell line were obtained from the Cell Bank of Chinese Academy of Science. Cells were maintained in RPMI 1640 medium (Gibco Industries, CA) with 10% fetal bovine serum (Gibco Industries) at 37°C in a humidified atmosphere with 5% CO_2. The Vincristine-resistant HCT8 cell (HCT8/VCR) was purchased from KEYGEN (KEYGEN, Suchou, China). Oxaliplatin-resistant HCT116 cell (HCT116/LOHP) were exposed to an initial oxaliplatin concentration of 0.1 μg/ml. The surviving population of cells was grown to 80% confluence and passaged twice over 9 days to ensure viability. The surviving population was then exposed to sequentially increased in the same manner to 0.5 μg/ml (15 days), 1.0 μg/ml (30 days), and finally to 2 μg/ml. The HCT8/VCR cells and HCT116/LOHP cells were seeded in the medium additionally contained 0.002 mg/ml VCR and 0.8 μg/ml LOHP, respectively, so as to maintain the drug-resistance phenotype and incubated in a drug-free medium for at least 1 week before use [Dallas et al., 2008; Sui et al., 2011].

TRANSIENT TRANSFECTION, VECTOR CONSTRUCTS, AND REPORTER GENE ASSAY

Cells were transfected using Oligofectamine reagent Lipofectamine^{TM}2000 (Invitrogen Corporation) with chemically synthesized double-stranded small interfering RNA (siRNA)s. The siRNA sequence of IGF-IR, MRP-2 and Nrf2 (denoted as si-IGF-IR, si-MRP-2, and si-Nrf2 hereafter for conciseness) and Scramble siRNA were in Supplementary Table SI. Several 5′-deletion constructs of the 1,229-bp fragment were generated for the functional characterization of the MRP-2 promoter. Primers of all vectors were in Supplementary Table SI. P-1229 (−1,229 to +30) and p-880 (−880 to +30) were inserted into PGL3-Basic vector and p-422 (−422 to −216) and p-422 mut ($^{-336}$AGACTGTGC to $^{-336}$AGAC**GAGAC**) were inserted into PGL3-promoter vector. The site-directed mutation was performed with TaKaRa MutanBEST Kit (TaKaRa Biotechnology Ltd., Shandong, China) following the manufacturer's protocol. A cDNA encoding human Nrf2 was generated by PCR from human brain cDNA library (Invitrogen Corporation). The coding region of Nrf2 cDNA was amplified by PCR using the primers containing KpnI and XhoI restriction sites and subcloned into vector pcDNA 3.1(+) to generate the construct pcDNA-Nrf2. The constructs were verified by DNA sequencing. Cell lysates were assayed for luciferase activity following the manufacturer's protocol (Promega Corporation), using a Centro XS3 LB960 microplate luminometer (Berthold Technol., Bad Wildbad, GER). Renilla luciferase activity was used to normalize the activity of firefly luciferase.

PROLIFERATION AND CHEMOSENSITIVITY ASSAY

Rates of proliferation and sensitivity to drugs were assessed using the colorimetric 3-(4,5-dimethylthiazol-2-yl)-2,5-diphenyltetrazolium bromide (MTT) assay as described previously[Liu et al., 2007]. All cells were seeded into 96-well culture plates ($2 \times 10^3 \times$ cells/well), respectively. The cells transfected with siRNAs were grown for 4 days. One plate was developed immediately after the medium change and other plates were developed every 24 h for 4 days. Assays were initiated by adding 20 μl of MTT substrate to each well and incubating the cells for an additional 3 h. Finally, the medium was removed and 200 μl DMSO was added to each well. Plates were read at a wavelength of 570 nm in an Automated Microplate Reader (Multiskan Ex, Lab systems, FIN). The chemosensitivity (growth inhibition) of anticancer drugs was expressed as IC_{50}. All cells were seeded into 96-well culture plates ($2 \times 10^3 \times$ cells/well), respectively. Cell growth was assessed after 72 h of exposure to 0–100 μg/ml of each anticancer drug. The IC_{50} value calculating was performed using GraphPad Prism5.0 software. All experiments were biologically repeated at least thrice to confirm consistency of the results obtained.

REAL-TIME QUANTITATIVE REVERSE TRANSCRIPTION-PCR ANALYSIS

Total RNA of siRNA or durgs treated cells was extracted using TRIZOL™ reagent (Promega Corporation) according to the supplier's instruction. Reverse transcription was done using Reverse Transcription System (TaKaRa Biotechnology Ltd.). Real-time PCR was performed using SYBR Green Supermix with an iCycler® thermal cycler (Bio-Rad Laboratories Inc., CA). Primers of all genes were in Supplementary Table SI. The data were collected and analyzed using the comparative C_t (threshold cycle) method using GADPH as the reference gene.

PROTEIN EXTRACTION AND WESTERN BLOTTING ANALYSIS

Cytoplasmatic and nuclear fractions, as well as total protein extracts were obtained as previously described[Xu et al., 2008]. Protein concentrations were determined using the BCA assay (Pierce Biotechnology Inc., Rockford). Equal amounts of proteins (50 μg) were prepared for Western blotting assay and resolved on 10% SDS–PAGE and electro-transferred onto PVDF membranes (Millipore, MA). After successful transfer of proteins, membranes were blocked for 1 h at room temperature and incubated with primary antibody in dilution buffer (BSA in TBS-T) overnight at 4°C. Membranes were then incubated with a secondary antibody alkaline phosphatase (AP) conjugated and detected in AP buffer containing NBT/BCIP at room temperature for 10–20 min, and then photographed. β-Actin and Lamin B were used as loading controls.

FLOW CYTOMETRIC ANALYSIS OF CELLULAR DNA CONTENT

Cells (6×10^4/well) were seeded in a six-well culture plate, transfected with 50 and 100 nM si-IGF-IR duplex for 72 h. Both floating and attached cells were collected and poured together in the centrifuge tubes. Cells were washed with phosphate-buffered saline (PBS), re-suspended and fixed in 70% ice-cold ethanol for 4 h at 4°C. Subsequently, they were treated with RNase A (50 μg/ml) for 30 min. Finally, cells were stained with propidium iodide (PI; 50 μg/ml) and analyzed in a FAC Scan flow cytometer (Becton Dickinson, NJ). The percentage of cells in G0/G1 phase, S phase, and G2/M phase was analyzed using standard ModiFit and CellQuest software programs.

FLOW CYTOMETRIC ANALYSIS OF APOPTOSIS AND NECROSIS

Extent of apoptosis was measured through Annexin VFITC apoptosis detection kit (Invitrogen Corporation) as described by the manufacturer's instruction. Briefly, cells (6×10^4/well) were seeded in six-well plates and transfected with siRNAs or treated with LOHP/VCR in two cell lines for 72 h. Cells were washed with cold PBS twice, gently resuspended in 400 μl 1 × binding buffer. Added 5 μl of Annexin V-FITC, gently vortex the cells and incubated for 10 min at 4–8°C in the dark. Add 10 μl of PI to tube for another 5 min at 4–8°C in the dark. And then it was analyzed by flow cytometry using FACScan flow cytometer (Becton Dickinson). Cells in the lower right quadrant represented early apoptosis and in the upper right quadrant represented late apoptotic cells.

FLUORESCENT MORPHOLOGICAL ASSAY

Cells (6×10^4/well) from exponentially growing cultures were seeded in six-well culture plate and transfected with siRNAs or treated with LOHP/VCR in two cell lines for 72 h. Cells were washed with PBS, fixed in MeOH-HOAc (3:1, v/v) for 10 min at 4°C, and stained with Hoechst 33258 (5 μg/ml in PBS) for 5 min at room temperature and then examined in a LEICA DMIRB fluorescent microscope at 356 nm.

MEASUREMENT OF INTRACELLULAR PLATINUM CONCENTRATION

Cells (6×10^4/well) were seeded in a six-well culture plate, transfected with 100 nM si-IGF-IR, si-MRP-2 or 1 μM SH-5 for 72 h and then HCT116/LOHP cells were incubated with 1 mg/L LOHP up to 120 min. After certain time points the medium was discarded quickly and the cells were washed three times with 5 ml ice-cold PBS buffer. Then cells were trypsinized, resuspended in fresh drug-free medium and centrifuged for 4 min at 4°C and $260 \times g$. The supernatant was discarded and the pellet was washed twice in 1 ml ice-cold PBS buffer. After centrifugation for 1 min at $6{,}000 \times g$ the supernatant was discarded again and the cell pellet was frozen at −20°C until analysis. Immediately, after thawing the cells were lysed with 200 ml concentrated nitric acid for 20 min on the water bath at 60°C. Then intracellular platinum concentrations were measured by flameless atomic absorption spectrometry (FAAS). The results were related to ng/10^6 measured by Casy™1 cell counter (Schärfe System, Reutlingen, GER).

HIGH-PERFORMANCE LIQUID CHROMATOGRAPHY ANALYSIS

Cells (6×10^4/well) were seeded in a six-well culture plate, transfected with 100 nM si-IGF-IR, si-MRP-2 or 1 μM SH-5 for 72 h and then HCT8/VCR cells were incubated with 1 mg/L VCR up to 120 min. High-performance liquid chromatography (Supelco Co Ltd, PA) analysis was performed on a 1200 system using a diamond C_{18} reversed-phase column (4.6 mm × 250 mm, 5 lm). The mobile phase consisted of methanol and water (55:45, v/v), potassium dihydrogen

phosphate (0.06 M) and adjusted to pH 5.0 at a flow rate of 0.8 ml/min. The sample volume injected was 20 μl. The detection wavelength was set at 297 nm.

STATISTICAL ANALYSIS

Statistical analyses were performed using Statistical Package for the Social Sciences software using the two-tailed Student's *t*-test. Significance was determined at the 95% confidence interval. All data were expressed as the mean ± standard deviation (SD) from a representative experiment.

RESULTS

EFFECT OF MULTIDRUG-RESISTANCE ON THE CELLULAR PHENOTYPE AND MDR MARKERS

P-gp, MRP-1, and MRP-2 were common biomarkers of MDR [Young et al., 2001; Sandusky et al., 2002]. High levels of putative MDR markers were detected in both MDR lines (Fig. 1).

MTT assay was used to evaluate sensitivity to chemotherapeutic agents. Four kinds of anticancer drugs, VCR (plant alkaloids and terpenoids), LOHP (alkylating agent), 5-Fluorouracil (5-FU, anti-metabolites), and Mitomycin C (MMC, cytotoxic antibiotics) were tested. These drugs exert anticancer effects through different mechanism. The IC_{50} values of each CRC cell lines are showed in Table I. HCT116/LOHP cells were resistant to LOHP as expected, but these cells also resistant to other kinds of anticancer drugs. Similarly, HCT8/VCR exhibited the same MDR phenotype.

TABLE I. IC_{50} Value of Two Multidrug-Resistant Colorectal Cancer Cell Lines and Their Parental Lines

IC_{50} value (μg/ml)	Cell lines			
	HCT-8/VCR	HCT8	HCT-116/L-OHP	HCT-116
Vincristine	42.72 ± 2.05	0.91 ± 0.06	23.34 ± 1.18	1.09 ± 0.12
Oxaliplatin	29.47 ± 1.46	0.86 ± 0.01	52.65 ± 2.69	1.13 ± 0.12
Fluorouracil	12.14 ± 1.59	0.82 ± 0.07	14.16 ± 2.99	1.01 ± 0.11
Mitomycin C	5.02 ± 0.26	0.3 ± 0.01	8.13 ± 0.21	0.67 ± 0.14

Multidrug-resistant colon cancer cell lines and their parental lines were treated with various concentrations of different anti-cancer drugs for 72 h and the IC_{50} value was calculated.

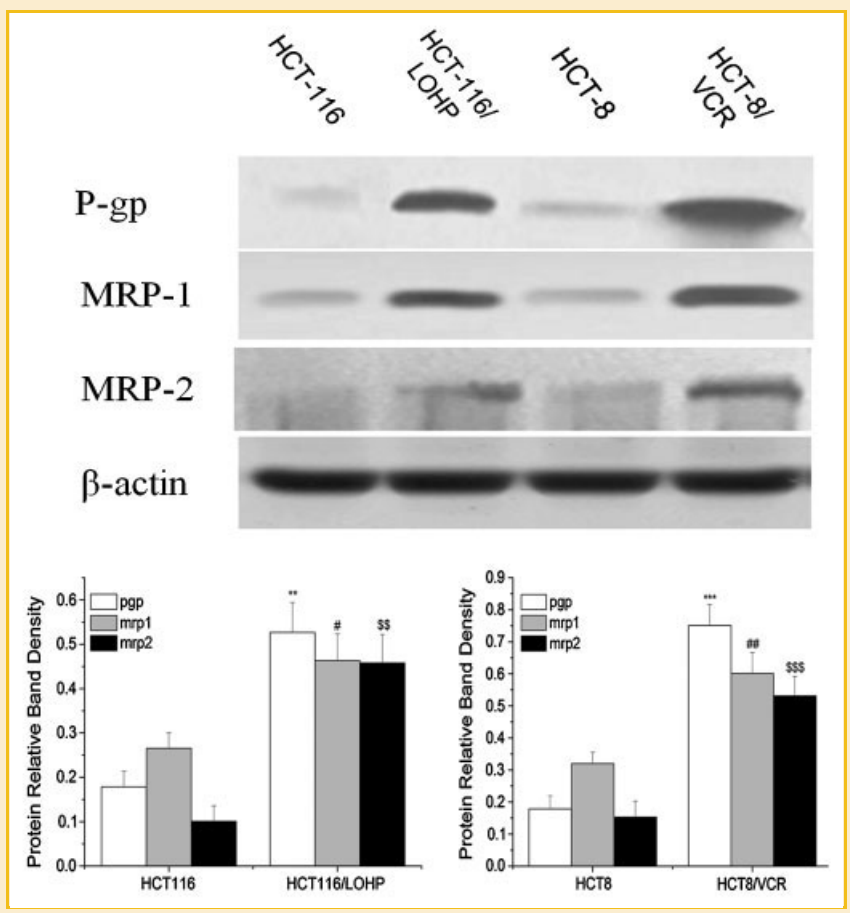

Fig. 1. Chemoresistant cell lines are enriched for MDR phenotype. Western blot analysis demonstrating the expression of multidrug-resistant putative biomarkers: P-gp, MRP-1, and MRP-2 in both drug resistant CRC cell lines compared to their parental lines. β-actin was used as a loading control. Scanning densitometry of the blots was used to quantify the Western blotting data. $^{**}P < 0.01$; $^{***}P < 0.001$, P-gp expression in MDR cells versus parental cells. $^{\#}P < 0.05$; $^{\#\#}P < 0.01$, MRP-2 expression in MDR cells versus parental cells. $^{\$\$}P < 0.01$; $^{\$\$\$}P < 0.001$, MRP-2 expression in MDR cells versus parental cells.

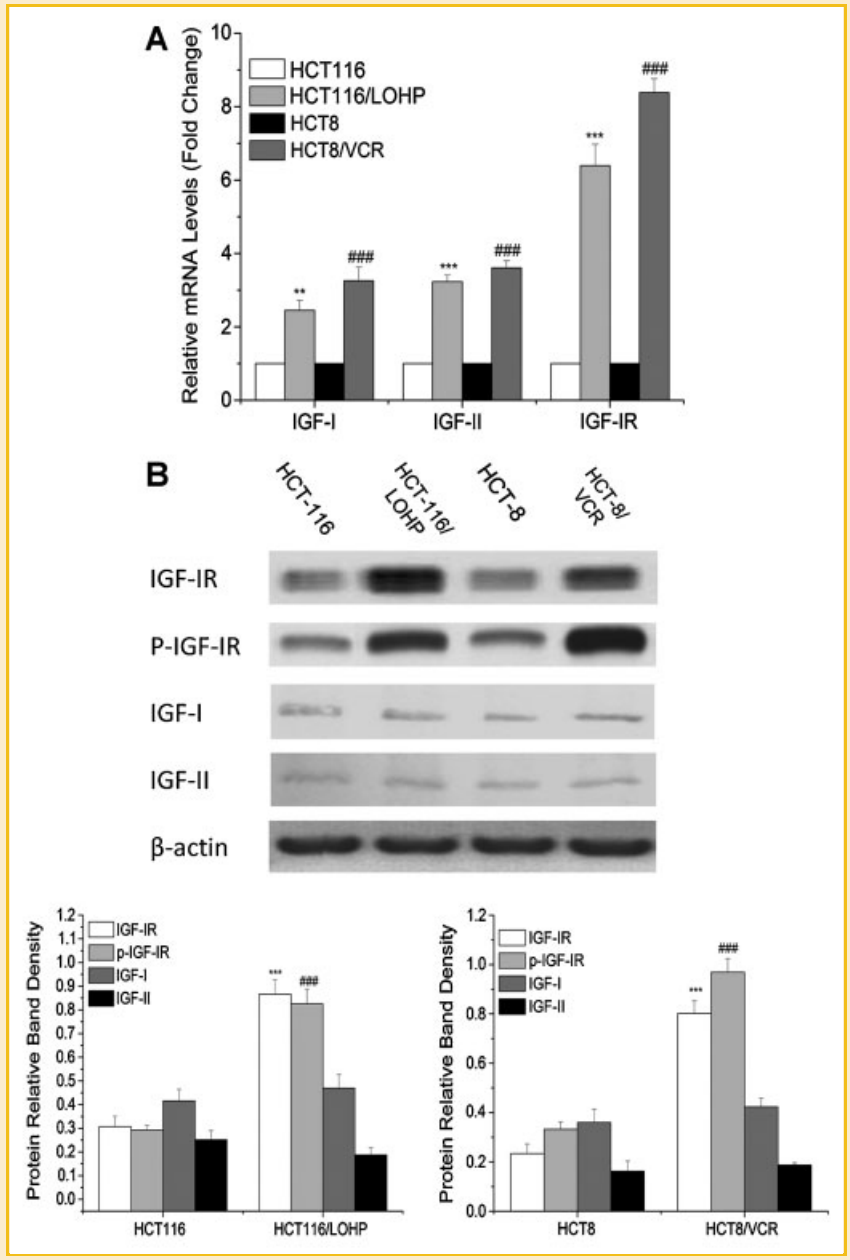

Fig. 2. mRNA and protein expression in four CRC cell lines. A: Quantification real-time reverse transcription-PCR was done on cDNA which was generated from total RNA. Quantification of the bands was performed and normalized change folds in relation to parental cells were shown in parenthesis. Significant differences from control were indicated by $^{**}P < 0.01$; $^{***}P < 0.001$, HCT116/LOHP versus HCT116. $^{\#\#\#}P < 0.01$, HCT8/VCR versus HCT8. B: Western blot analysis demonstrating the expression of IGF-I, IGF-II and IGF-IR (total and phosphorylation) in both drug resistant CRC cell lines compared to their parental lines. β-actin was used as a loading control. Scanning densitometry of the blots was used to quantify the Western blotting data. $^{***}P < 0.001$, IGF-IR expression in MDR cells versus parental cells. $^{\#\#\#}P < 0.001$, pIGF-IR expression in MDR cells versus parental cells. All data were presented as means ± SD and as representative of an average of three independent experiments.

EXPRESSION OF IGF-I, IGF-II, AND IGF-IR IN HUMAN COLORECTAL CELLS

To study the functional activity of IGF-IR in resistant/unresistant CRC cells, RT-PCR, and Western blotting were performed after cell harvest. As showed in Figure 2, the mRNA levels of IGF axis were all significant higher in both MDR cell lines than in their parental lines. However, IGF-IR and p-IGF-IR, not IGF-I or IGF-II, protein overexpression was found in both MDR cells. The observations indicating that overexpression of IGF-IR may play a role in CRC cell multidrug-resistant process.

EFFECTS OF IGF-IR INHIBITION ON CELL GROWTH

To obtain the role IGF-IR plays in the multidrug resistant process, chemical synthesis siRNAs were employed to disrupt IGF-IR expression. Cells proliferation was assessed by plating equal numbers of cells of each cell line and by using MTT assay as an

index of cell number. The cell growth curve showed that disruption of the IGF-IR may inhibit the MDR cells proliferation significantly. The cell growth curve demonstrated that MDR cells proliferation were inhibited notably in at a time-dependent manner after si-IGF-IR treated, and the highest inhibitory was 45% in HCT8/VCR cells ($P < 0.001$) and 40% in HCT116/LOHP cells ($P < 0.001$), respectively (Fig. 3A). No significant differences in cellular proliferation were detected between untreated or scrambled treated cells. Two parental lines were also inhibited most at 72 h (data not shown) and the highest inhibitory was 15% and 11% in HCT8 and HCT116 cells, respectively (Fig. 3B).

To gain insights into the mechanism by which anti-proliferation effect was achieved in MDR cells, we investigated the effect on cell cycle distribution by fluorescence-activated cell sorting (FACS) analysis. Both types' cells were accumulated in G2/M phase when IGF-IR was deficient. Furthermore, a dose dependent effect was found in si-IGF-IR caused cycle arrest (Fig. 3C). IGF-IR down-regulation resulted in a less significant accumulation in G2/M phase in parental lines (Supplementary Fig. S1A). The results indicated that IGF-IR might serve as a more specific modulator in MDR CRC cells.

EFFECT OF IGF-IR INHIBITION ON REVERSAL OF THE DRUG-RESISTANT PHENOTYPE

To further characterize the effect of IGF-IR on MDR cancer cells, Cells were transfected with si-IGF-IR and then treated with anticancer drugs in two MDR lines. Because the growth rate of both kinds of cells was inhibited highest in 72 h, cells were treated with drugs for 72 h after transfection to evaluate the effect of siRNA. The IC_{50} value of cells transfected with si-IGF-IR was showed in Table II. Si-IGF-IR caused a significant reduction in every IC_{50} in transfected cells compared to control, suggesting that inhibition of IGF-IR may increase drug sensitivity. Increasing drug sensitivity was also found in MRP-2 disrupted cells. Interestingly, the 5-FU IC_{50}

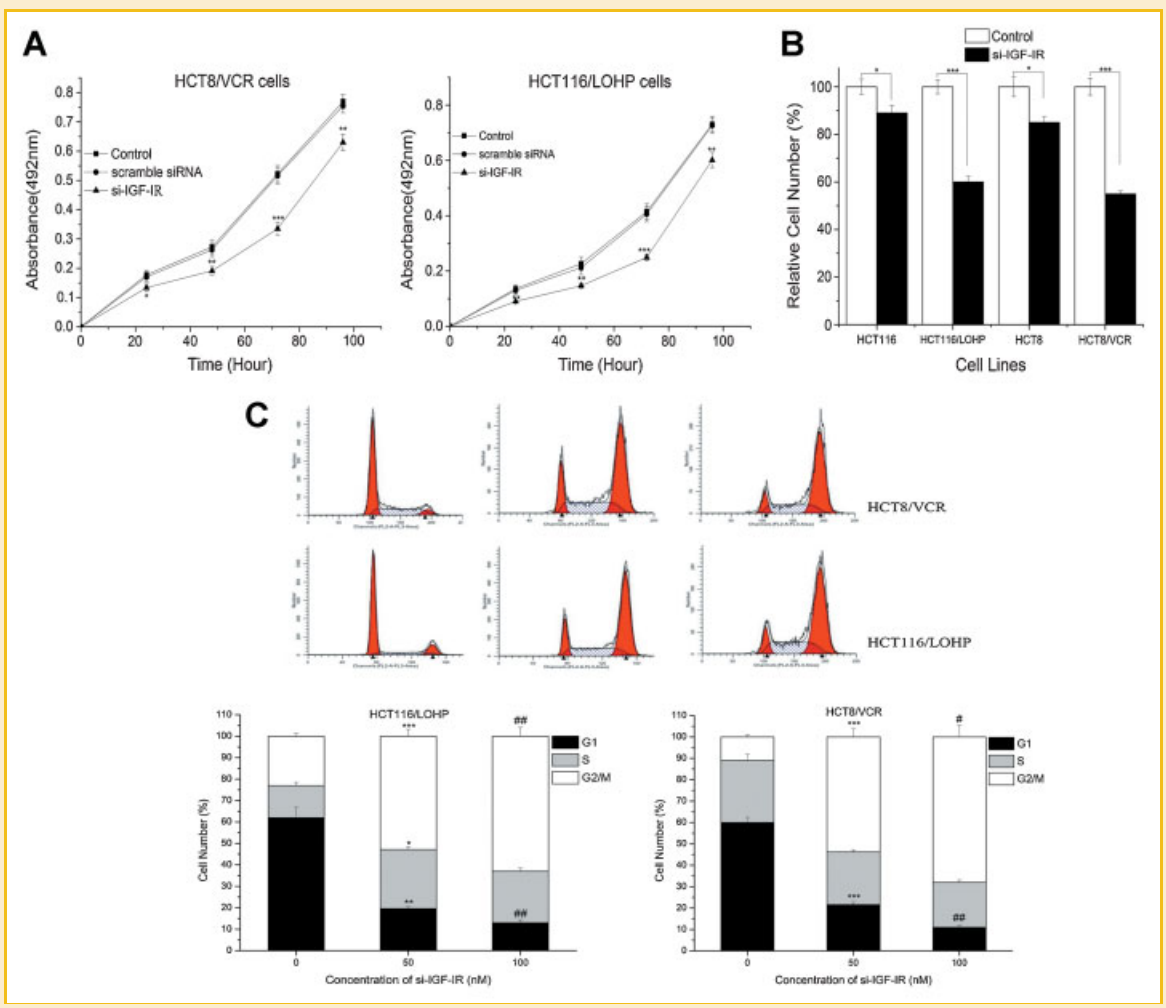

Fig. 3. Cell growth inhibition and cell cycle arrest. Four lines were transfected with a 100 nM si-IGF-IR and scramble siRNA duplex. The results of the inhibitory rates of cell growth were measured by MTT assay. A: Two MDR lines were transfected with 100 nM si-IGF-IR for 96 h and the inhibitory was also measured by MTT assay. B: 72 h inhibitory rates of siRNA treated lines were tested. Significant differences from control were indicated by $^{*}P < 0.05$; $^{**}P < 0.01$; $^{***}P < 0.001$. C: Cells transfected with 50 and 100 nM si-IGF-IR for 72 h were assessed using propidium iodide (PI) staining with flow cytometry. $^{**}P < 0.01$; $^{***}P < 0.001$, 50 nM si-IGF-IR treated cells versus control cells. $^{\#}P < 0.05$; $^{\#\#}P < 0.01$, 100 nM si-IGF-IR treated cells versus 50 nM treated cells. All data were expressed as means ± SD of three separate experiments. [Color figure can be seen in the online version of this article, available at http://wileyonlinelibrary.com/journal/jcb]

TABLE II. Effects of si-IGF-IR and si-MRP2 on Drug Sensitivity of HCT8/VCR and HCT116/LOHP Cells

IC_{50} value (μg/ml)	Vincristine	Oxaliplatin	Fluorouracil	Mitomycin C
HCT8/VCR	42.72 ± 2.05	29.47 ± 1.46	12.14 ± 1.59	5.02 ± 0.26
Si-IGF-IR treated	$18.64 \pm 2.01^{***}$	$11.16 \pm 1.11^{***}$	$5.23 \pm 1.08^{**}$	$2.12 \pm 0.11^{***}$
Si-MRP2 treated	$12.43 \pm 2.01^{\#\#\#}$	$10.63 \pm 0.98^{\#\#\#}$	10.26 ± 1.33	$2.43 \pm 0.14^{\#\#\#}$
SH-5 treated	$23.26 \pm 1.97^{\$\$\$}$	$15.63 \pm 1.24^{\$\$\$}$	$7.74 \pm 1.11^{\$}$	$3.26 \pm 0.19^{\$\$}$
HCT116/LOHP	23.34 ± 1.18	52.65 ± 2.69	14.16 ± 2.99	8.13 ± 0.21
Si-IGF-IR treated	$12.45 \pm 1.61^{***}$	$19.94 \pm 1.23^{***}$	$6.63 \pm 1.29^{*}$	$3.01 \pm 0.13^{***}$
Si-MRP2 treated	$10.16 \pm 1.16^{\#\#\#}$	$17.22 \pm 1.18^{\#\#\#}$	11.89 ± 1.82	$4.2 \pm 0.17^{\#\#\#}$
SH-5 treated	$15.87 \pm 1.88^{\$\$}$	$23.95 \pm 1.92^{\$\$\$}$	$7.88 \pm 1.62^{\$}$	$3.68 \pm 0.25^{\$\$\$}$

Cells were exposed to anticancer drugs for 72 h after treatment with specific siRNA (100 nM) and IC_{50} (μM drug concentration inhibiting 50% growth) was determined by MTT assay. Values are means ± SD of three experiments.
$^{*}P < 0.05$.
$^{**}P < 0.01$.
$^{***}P < 0.001$, si-IGF-IR treated cells versus untreated cells.
$^{\#\#\#}P < 0.001$, si-MRP2 treated cells versus untreated cells.
$^{\$}P < 0.05$.
$^{\$\$}P < 0.01$.
$^{\$\$\$}P < 0.001$, SH-5 treated cells versus untreated cells.

were found decreased significantly in si-IGF-IR cells but not in si-MRP-2 treated cells.

To determine whether IGF-IR inhibition may lead to cells apoptosis or contribute to drugs induced cells apoptosis, an assay combining annexin V and propidium iodide were performed. As assessed by flow cytometry, the fraction of apoptotic increased slightly when treated with 100 nM si-IGF-IR or drugs in two lines, respectively, however, notable apoptosis was found in co-treated cells (Fig. 4A).

To confirm the flow cytometry, cells were stained with Hoechst 33258. An intact nuclear structure was observed in the control cells; In contrast, all treated cells had chromosomal condensation and formation of apoptotic bodies and the most obvious phenomenon was observed in co-treated group (Fig. 4B).

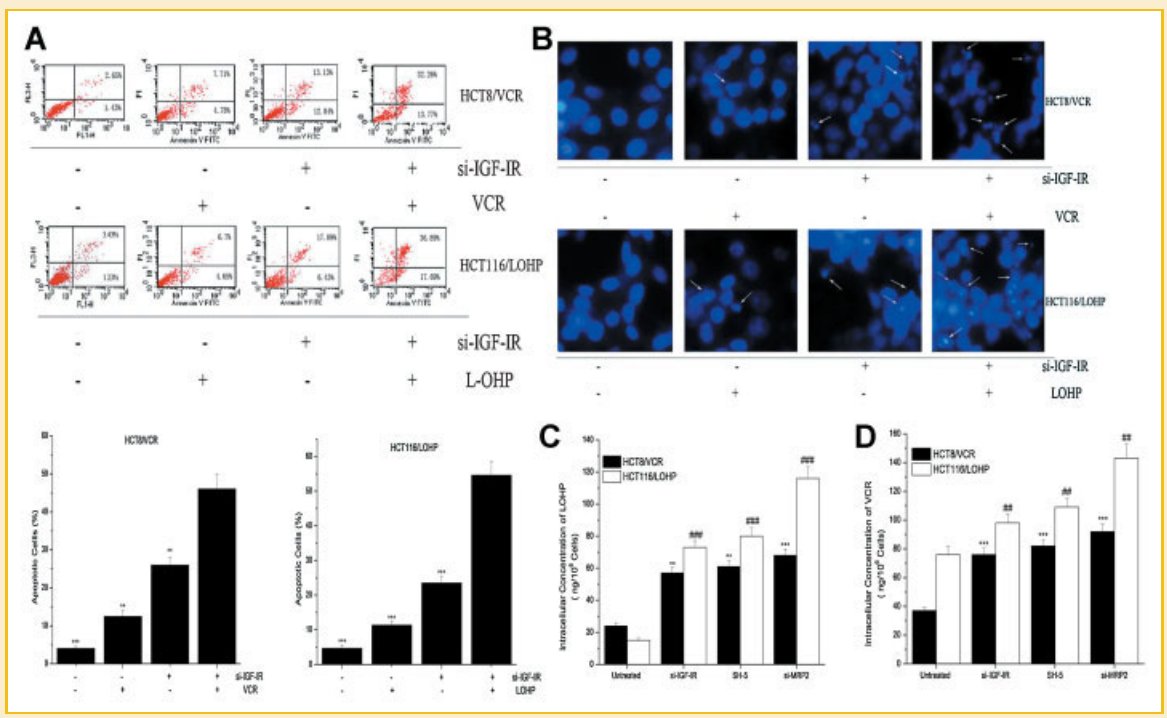

Fig. 4. Effect of si-IGF-IR on VCR or LOHP-treated cells. 100 nM si-IGF-IR transfected cells were treated with 21 μg/ml VCR or 26 μg/ml LOHP (1/2 IC_{50}) for 72 h (A) apoptosis were assessed using Annexin V-FITC analysis. $^{**}P < 0.01$; $^{***}P < 0.001$, control or si-IGF-IR or drugs treated group versus si-IGF-IR and drugs co-treated group. B: Fluorescent staining of nuclei by Hoechst 33258. Condensed and fragmented nuclei and apoptotic bodies were noted with arrows. All data were expressed as means ± SD of three separate experiments. Transfected cells were treated with 1 mg/L VCR or LOHP for 2 h (C) a FAAS method was used to detect intracellular platinum concentration and (D) a HPLC method was used to detect intracellular VCR concentration. $^{**}P < 0.01$; $^{***}P < 0.001$, si-IGF-IR (100 nM), SH-5 (1 μM), or si-MRP-2 (100 nM) treated group versus untreated group of HCT8/VCR cells. $^{\#\#}P < 0.01$; $^{\#\#\#}P < 0.001$, si-IGF-IR (100 nM), SH-5 (1 μM) or si-MRP-2 (100 nM) treated group versus untreated group of HCT116/LOHP cells. [Color figure can be seen in the online version of this article, available at http://wileyonlinelibrary.com/journal/jcb]

To confirm the chemosensitivity was eventually due to increased intracellular drug concentration, HPLC and FAAS were performed to measure intracellular VCR and LOHP concentration. In agreement with the observations in IC_{50}, the intracellular concentration of VCR and LOHP were significantly increased after si-IGF-IR and si-MRP-2 treated (Fig. 4C,D), revealed that IGF-IR disruption may induce drug accumulation through MRP-2 suppression in MDR cells.

Taken together, these results suggest that the IGF-IR could play an essential role in pro-survival and anti-apoptotic pathways in MDR cancer cells. Inhibition of IGF-IR may cause increasing drug sensitivity through drug accumulation, therefore induce cell apoptosis in a lower dosage.

EFFECT OF IGF-IR INHIBITION ON GROWTH FACTOR RECEPTOR DOWNSTREAM PATHWAY

To obtain a clue towards understanding the mechanisms of IGF-IR signaling regulating the multidrug-resistant phenotype, cells treated with si-IGF-IR or drugs were assessed by Western blot analysis. We evaluated the consequence of inhibition of IGF-IR by using AKT, pAKT, and Nrf2 as molecular surrogates of downstream IGF-IR signaling. As show in Figure 5A, si-IGF-IR induced down-regulation of IGF-IR. The decrease in IGF-IR is associated with decrease in pAKT and nucleolus Nrf2. Not only MRP-2 but other MDR transporter such as P-gp and MRP-2 were also down-regulated after IGF-IR inhibition. IGF-IR may also modulate other MDR transports and might serve as a de novo wide spread MDR

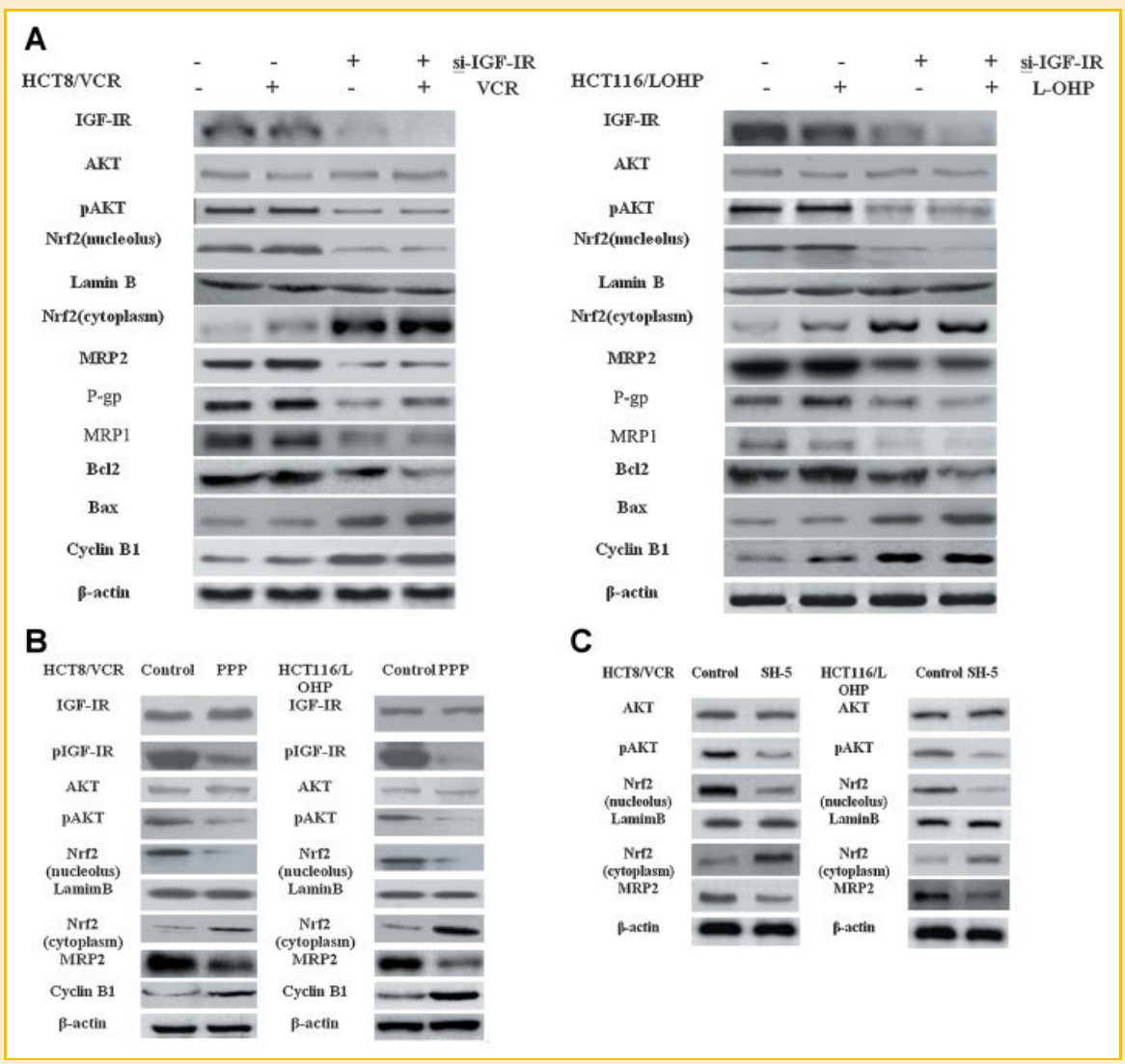

Fig. 5. The alternation of AKT/Nrf2/ARE/MRP-2 pathway downstream of IGF-IR. A: 100 nM transfected cells were treated with 21 μg/ml VCR or 26 μg/ml LOHP for 72 h. HCT-116/L-OHP cells and HCT-8/VCR cells were analyzed using Western blotting. β-actin and Lamin B were used as loading controls. Western blots were representative of three independent experiments. B: Two MDR cell lines were treated with 1 μM IGF-IR-specific inhibitor PPP for 72 h. C: Two MDR cell lines were treated with 1 μM AKT-specific inhibitor SH-5 for 72 h. Western blotting assay was also performed. β-actin and Lamin B were used as loading controls.

modulator. Si-IGF-IR induces a notable increase and decrease in the apoptotic related protein Bax and Bcl2, respectively. Furthermore, IGF-IR induces a notable increase in the cell-cycle regulatory protein cyclin B1. The effect of si-IGF-IR on the cell cycle regulatory protein is consistent with the occurrence of G2/M-phase cell-cycle arrest. Consistent with previous study, overexpression of Nrf2 was found in MDR cells (Supplementary Fig. S1B).

To control the specificity of IGF-IR, an AKT inhibitor SH-5 was used. SH-5 (1 μM) also increased the drug sensitivity (Table II). The HPLC assay and FAAS assay showed there was higher intracellular drug concentration in SH-5 treated cells compared to untreated cells (Fig. 4C,D). It suggested that effects on drug sensitivity might not be a secondary effect to the decreased proliferation and cell-cycle arrest observed upon IGF-IR knock-down.

A specific inhibitor of IGF-IR by PPP was also used to confirm some of the results and to rule out the possibility of nonspecific effects of the si-IGF-IR. PPP (1 μM) induces marked down-regulation of pIGF-IR, without a noticeable change in IGF-IR levels. PPP decreased pAkt, nuclear Nrf2, and MRP-2 levels (Fig. 5B).

We next investigated the effect of the si-IGF-IR on nuclear translocation of Nrf2 and expression of MRP-2. The result showed that the expression of MRP-2 and nuclear translocation of Nrf2 reduced after si-IGF-IR or SH-5 (Fig. 5C) treatment, which also confirms the specific effects of si-IGF-IR. These finding strongly suggest that IGF-IR may functionally specifically regulate MRP-2 expression.

EFFECT OF IGF-IR INHIBITION ON MRP-2 PROMOTER

To determine whether the 5′-flanking region of the MRP-2 gene contains the sequences that mediate the si-IGF-IR induction of the MRP-2 gene, HCT8/VCR, and HCT116/LOHP cells were transfected with either the construct containing two ARE-like elements (p-1229) or one ARE-like element (p-880). The reporter activity of both constructs was measured in cell extracts. The data showed a significantly decrease in p-1229 and p-880 promoter activity but no significant difference between them after si-IGF-IR treatment. We hypothesized that the first ARE-like element ($^{-1098}$GTGACAGTA) may not be involved in IGF-IR regulation.

To investigate whether the second ARE-like element ($^{-336}$AGACTGTGC) was indeed involved in the induction of si-IGF-IR treatment, two reporter vectors were constructed. We inserted DNA containing sequence −422 to −328 nt of the MRP-2 into pGL3-promoter vector which contains a basal promoter from SV40. Recombinant DNA containing mutant ARE-like site ($^{-336}$AGACGAGAC) was similarly constructed. Figure 6A shows that mutation at the Nrf2-binding site abolished the induction of reporter expression by si-IGF-IR, whereas the wild-type construct remained responsive to the induction by the putative oncogene. Reporter expression in pcDNA-Nrf2 treated cells was significantly increased compared to untreated cells. Therefore, the inhibition of PI3K/Akt signaling by si-IGF-IR may downregulate Nrf2-ARE-like-dependent transcriptional activity, resulting in the suppression of the MRP-2 promoter activity. The effect of si-IGF-IR was also confirmed in

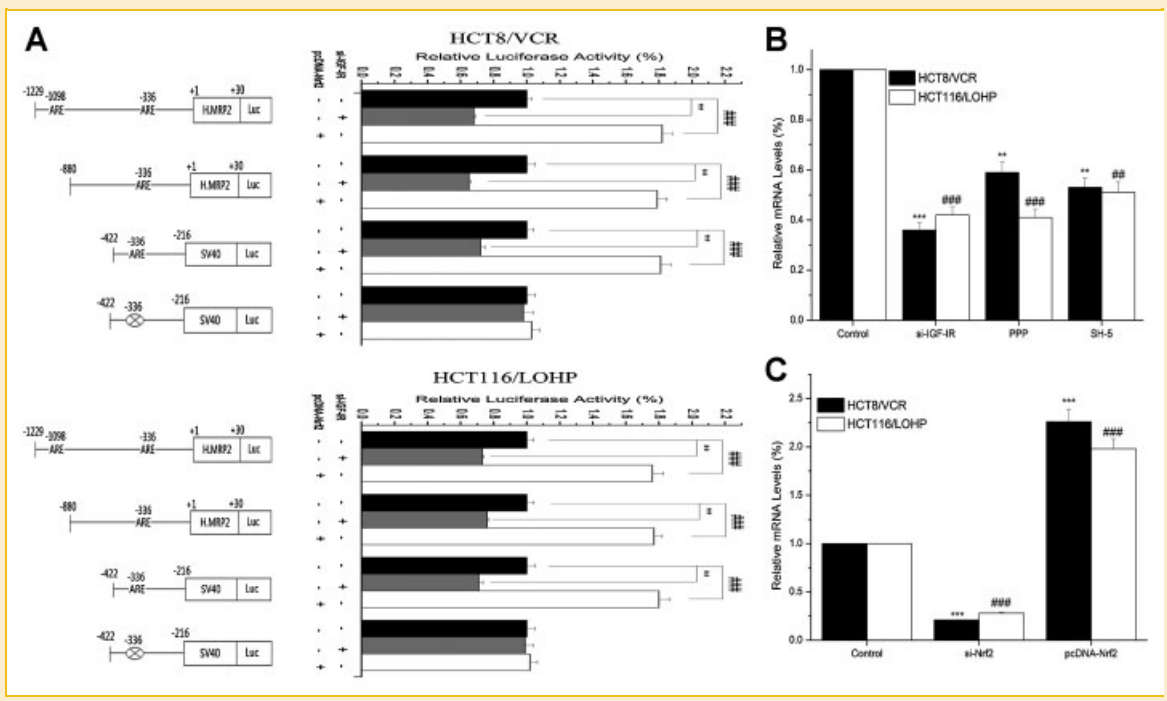

Fig. 6. Mechanism of reversal of MDR phenotype after IGF-IR signaling blockade. A: 1,229 and 880 bp fragments of 5′-flanking region of MRP-2 were cloned into PGL3-Basic vector and wild and mutated type of second ARE-like element (−422 to −216) were inserted into PGL3-Promoter vector. All vectors were transfected into two MDR cell lines then treated with si-IGF-IR and pcDNA-Nrf2 and the luciferase activity were assayed. B: Real-time PCR analysis were performed to detect the MRP-2 mRNA level after si-IGF-IR (100 nM), SH-5 (1 μM) and PPP (1 μM) treated in two lines for 72 h. $^{**}P < 0.01$; $^{***}P < 0.001$, si-IGF-IR or PPP treated HCT8/VCR cells versus untreated cells. $^{\#\#\#}P < 0.001$, si-IGF-IR or PPP treated HCT116/LOHP cells versus untreated cells. C: MRP-2 mRNA level after si-Nrf2 (100 nM) and pcDNA-Nrf2 treated in two lines. $^{**}P < 0.01$; $^{***}P < 0.001$, si-Nrf2 or pcDNA-Nrf2 treated HCT8/VCR cells versus untreated cells. $^{\#\#\#}P < 0.001$, si-Nrf2 or pcDNA-Nrf2 treated HCT116/LOHP cells versus untreated cells.

mRNA levels. The real-time PCR analysis showed that MRP-2 mRNA level was also reduced when IGF-IR signaling was blocked in both cell lines (Fig. 6B) and MRP-2 mRNA level was increased when treated with pcDNA-Nrf2 (Fig. 6C), which also suggested the effect of Nrf2 in regulating MRP-2 transcribing.

DISCUSSION

In the present study, two MDR CRC cell lines were employed as our cell models. In these models, the putative multidrug-resistant biomarker P-gp, MRP-1, and MRP-2 were overexpressed in MDR lines as observed. Higher IC_{50} values of four kinds of antitumor drugs were also found in sub-cell-lines compared to their parental lines.

Both sub-cell-lines were significantly enriched for IGF-IR mRNA and protein. Although IGF-IR has been described as an oncogen in many different types of cancer, it is unclear whether MDR is caused by a direct effect of IGF-IR signaling. It still remains unknown how the increase of IGF-IR expression in these cells works precisely. One possibility is that the strong expression of IGF-IR helps cells activate the downstream signal transduction pathway such as PI3K/AKT pathway to against apoptosis and enhance cell proliferation. According to above data, IGF-IR may play a role in multidrug-resistant cancer cells.

IGF-IR disruption significantly inhibits the growth rate in both MDR cells lines but slightly in parental lines, which indicated that IGF-IR may play a more specific role in the process of regulating MDR CRC cells. Cell cycle is accumulated in G2/M phase when IGF-IR pathway is blockade, consistent with previous study [Amin et al., 2010]. Connections between the PI3K/Akt and cyclin B1 are well known [Roberts et al., 2002; Strömberg et al., 2006], and it is reasonable to suggest that the G2/M-phase accumulation induced by IGF-IR is due to an increase of the cyclin B1. The protein alterations are in agreement with the occurrence of G2/M-phase cell-cycle arrest.

Since IGF-IR has been proved important in MDR cells, we postulate that IGF-IR inhibition may contribute to reverse the MDR phenotype. IGF-IR silenced MDR cells were then treated with anticancer drugs we used before. The IC_{50} value indicates that drug sensitivity is increased by IGF-IR disruption. PI/FITC flow cytometry analysis showed that total apoptosis rate were significantly higher in co-treated group compared to other groups and Hoechst stain experiment confirmed the pro-apoptotic ability of si-IGF-IR. HPLC and FAAS data explored that si-IGR-IR may increase intracellular VCR and LOHP concentration, consistent with our postulation. Therefore, according to above deducing, the silencing of the IGF-IR gene caused by RNAi may help increasing drug sensitivity in human colorectal carcinoma cells.

But the effects on drug sensitivity might be a secondary effect of the decreased proliferation and cell-cycle arrest observed upon IGF-IR knock-down. To control the specificity of IGF-IR inhibition, AKT-specific inhibitor SH-5 was used. The MTT assay showed that SH-5 acted similarly as si-IGF-IR. The results were also confirmed by HPLC assay and FAAS assay.

MRP-2 is a member of ABC superfamily. As reported, MRP-2 can pump glutathione associated anticancer drugs such as LOHP and VCR out of cells. Hypothesis may be drawn that MRP-2 would be involved in the IGF-IR mediated chemoresistance. Our data reveal that si-IGF-IR act the same as si-MRP-2 and suggests that the chemosensitivity induced by si-IGF-IR may through MRP-2 regulation. However, IC_{50} of 5-FU were reduced significantly in si-IGF-IR but not in si-MRP-2 treated MDR cells in our result. These findings led to another hypothesis that there is an alternative mechanism contributing to the increase of chemosensitivity to 5-FU in two MDR cell lines when IGF-IR is disrupted. The hypothesis requires further study in preclinical and clinical trials.

The promoter region of human MRP-2 has been cloned and several potential transcriptional start sites have been identified. There are two ARE-like elements in the promoter region[Stöckel et al., 2000]. The increase of chemosensitivity may be due to the MRP-2 down expression which is caused by nuclear translocation of Nrf2. It led to our examination of the mechanism behind it. According to our data, in two MDR cell lines, the phosphorylation of AKT decreased in all IGF-IR reduction circumstances. AKT is also an important factor in regulating cell proliferation which may be the reason of growth inhibition[Ericson et al., 2009]. As a downstream factor of PI3K/AKT pathway [Gallagher and LeRoith, 2010; Kloo et al., 2011], the expression of nucleolus Nrf2 is proportional to the pAKT level. It cannot be completely excluded that the effect of si-IGR-IR is due to a direct regulation on AKT/Nrf2. To rule out the off-target effect in RNA interference, an IGF-IR-specific inhibitor PPP was performed. PPP also induced a marked decrease in MRP-2 expression through AKT/Nrf2 regulation, which provides strong evidence to support a direct role of IGF-IR in regulating MRP-2. The intensity of two MRP-2 promoter luciferase vectors, one contains two ARE-like elements (p-1229) and another contains one ARE-like element (p-880), were treated with si-IGF-IR or pcDNA-Nrf2. The data revealed that IGF-IR inhibition may lead to a low MRP-2 transcribing through the second ARE-like element and vice versa. We therefore constructed other two vectors. One contains a wild type second ARE-like element while another contain a mutated one. Luciferase activity decreased in wild-type ARE-like expressed cells. It may be caused by IGF-IR silencing mediated MRP-2 promoter repression. Real-time PCR analysis confirmed the finding. These findings strongly suggested the direct role for IGF-IR in regulating MRP-2.

VCR and LOHP have distinct mechanisms to cause tumor cell cytotoxicity. It is unlikely that the acquired chemoresistance to these agents yield common molecular alterations. However, our data show that when cells are chronically exposed to either agent, the resulting cells acquire similar molecular alterations. Interestingly, these drug resistance cells expressed increased levels of IGF-IR (and phosphorylated IGF-IR), making these cells more sensitive to blockade of this gene. Recent data have suggested that targeting of growth factor receptors or downstream pathway may inhibit cancer cell survival, cell growth [Manning and Cantley, 2007; Düvel et al., 2010; Li et al., 2010] and even be an effective method for multidrug-resistant CRCs [Boccaccio and Comoglio, 2006].

The knowledge that small RNAs can affect gene expression has had a tremendous impact on basic and applied research. In the meanwhile, RNAi is currently one of the most promising new approaches for disease therapy. The enormous interest in this

phenomenon ensures that we will soon witness fast advances and new applications for RNAi-based therapies [Castanotto and Rossi, 2009].

In conclusion, herein a new role for IGF-IR in colorectal MDR cancer cells is identified. In detail, IGF-IR silencing may increase anticancer drugs sensitivity through MRP-2 transcribes inhibition. These findings are expected to expand current understanding of the biology of IGF-IR and MDR. The possibility of a significant role of IGF-IR in vivo also needs to be extensively investigated. As targeting of IGF-IR signaling is currently being examined in clinical trials, the identified role of IGF-IR in MDR may have a significant therapeutic impact on the treatment of such disease in the near future.

ACKNOWLEDGMENTS

This work was supported by the Fundamental Research Funds for the Central Universities, Shanghai Leading Academic Discipline Project (Project No. B507) and 111 Project, Grant No. B07023.

REFERENCES

Amin HM, Shi P, Lai R, Lin Q, Iqbal AS, Young LC, Kwak LW, Ford RJ. 2010. IGF-IR tyrosine kinase interacts with NPM-ALK oncogene to induce survival of T-cell ALK(+) anaplastic large-cell lymphoma cells. Blood 114:360–370.

Boccaccio C, Comoglio PM. 2006. Invasive growth: A MET-driven genetic programme for cancer and stem cells. Nat Rev Cancer 6:637–645.

Castanotto D, Rossi JJ. 2009. The promises and pitfalls of RNA-interference-based therapeutics. Nature 457:426–433.

Chakraborty AK, Welsh A, DiGiovanna MP. 2010. Co-targeting the insulin-like growth factor I receptor enhances growth-inhibitory and pro-apoptotic effects of anti-estrogens in human breast cancer cell lines. Breast Cancer Res Treat 120:327–335.

Cui Y, König J, Buchholz U, Spring H, Leier I, Keppler D. 1999. Drug Resistance and ATP-dependent conjugate transport mediated by the apical multidrug resistance protein, MRP2, permanently expressed in human and canine cells. Mol Pharmacol 55:929–937.

Dallas NA, Xia L, Fan F, Yang AD, Gray MJ, Samuel S, Gaur P, Ellis LM. 2008. Chemo-resistant colorectal cancer cells are enriched for tumor stem cells and sensitive to IGF-1R inhibition. J Am Coll Surg 207:S99.

Dallas NA, Xia L, Fan F, Gray MJ, Gaur P, van Buren G, Samuel S, Kim MP, Lim SJ, Ellis LM. 2009. Chemoresistant colorectal cancer cells, the cancer stem cell phenotype, and increased sensitivity to insulin-like growth factor-I receptor inhibition. Cancer Res 69:1951–1957.

Düvel K, Yecies JL, Menon S, Raman P, Lipovsky AI, Souza AL, Triantafellow E, Ma Q, Gorski R, Cleaver S, Vander Heiden MG, MacKeigan JP, Finan PM, Clish CB, Murphy LO, Manning BD. 2010. Activation of a metabolic gene regulatory network downstream of mTOR complex 1. Mol Cell 39:171–183.

Ericson K, Gan C, Cheong I, Rago C, Samuels Y, Velculescu VE, Kinzler KW, Huso DL, Vogelstein B, Papadopoulos N. 2009. Genetic inactivation of AKT1, AKT2, and PDPK1 in human colorectal cancer cells clarifies their roles in tumor growth regulation. Proc Natl Acad Sci USA 107:2598–2603.

Gallagher EJ, LeRoith D. 2010. The proliferating role of insulin and insulin-like growth factors in cancer. Trends Endocrin Met 21:610–618.

Garrouste F, Remacle-Bonnet M, Fauriat C, Marvaldi J, Luis J, Pommier G. 2002. Prevention of cytokine-induced apoptosis by insulin-like growth factor-I is independent of cell adhesion molecules in HT29-D4 colon carcinoma cells—Evidence for a NF-kappa B-dependent survival mechanism. Cell Death Differ 9:768–779.

Haimeur A, Conseil G, Deeley RG, Cole SP. 2004. The MRP-related and BCRP/ABCG2 multidrug resistance proteins: Biology, substrate specificity and regulation. Curr Drug Metab 5:21–53.

Hart LS, Dolloff NG, Dicker DT, Koumenis C, Christensen JG, Grimberg A, El-Deiry WS. 2011. Human colon cancer stem cells are enriched by insulin-like growth factor-1 and are sensitive to figitumumab. Cell Cycle 10:2331–2338.

Hopkins A, Crowe P, Yang J-L. 2010. Effect of type 1 insulin-like growth factor receptor targeted therapy on chemotherapy in human cancer and the mechanisms involved. J Cancer Res Clin Oncol 136:639–650.

Kauffmann H-M, Pfannschmidt S, Zöller H, Benz A, Vorderstemann B, Webster JI, Schrenk D. 2002. Influence of redox-active compounds and PXR-activators on human MRP1 and MRP2 gene expression. Toxicology 171:137–146.

Kloo B, Nagel D, Pfeifer M, Grau M, Düwel M, Vincendeau M, Dörken B, Lenz P, Lenz G, Krappmann D. 2011. Critical role of PI3K signaling for NF-κB-dependent survival in a subset of activated B-cell-like diffuse large B-cell lymphoma cells. Proc Natl Acad Sci USA 108:272–277.

Li S, Brown MS, Goldstein JL. 2010. Bifurcation of insulin signaling pathway in rat liver: mTORC1 required for stimulation of lipogenesis, but not inhibition of gluconeogenesis. Proc Natl Acad Sci USA 107:3441–3446.

Liu JW, Yang F, Zhang Y, Li JY. 2007. Studies on the cell-immunosuppressive mechanism of Oridonin from Isodon serra. Int Immunopharmacol 7:945–954.

Maher JM, Aleksunes LM, Dieter MZ, Tanaka Y, Peters JM, Manautou JE, Klaassen CD. 2008. Nrf2- and PPARα-mediated regulation of hepatic Mrp transporters after exposure to perfluorooctanoic acid and perfluorodecanoic acid. Toxicol Sci 106:319–328.

Manning BD, Cantley LC. 2007. AKT/PKB signaling: Navigating downstream. Cell 129:1261–1274.

Min Y, Adachi Y, Yamamoto H, Imsumran A, Arimura Y, Endo T, Hinoda Y, Lee CT, Nadaf S, Carbone DP, Imai K. 2005. Insulin-like growth factor I receptor blockade enhances chemotherapy and radiation responses and inhibits tumour growth in human gastric cancer xenografts. Gut 54:591–600.

Natrajan R, Reis-Filho JS, Little SE, Messahel B, Brundler M-A, Dome JS, Grundy PE, Vujanic GM, Pritchard-Jones K, Jones C. 2006. Blastemal expression of Type I insulin-like growth factor receptor in Wilms' Tumors is driven by increased copy number and correlates with relapse. Cancer Res 66:11148–11155.

Ohta T, Iijima K, Miyamoto M, Nakahara I, Tanaka H, Ohtsuji M, Suzuki T, Kobayashi A, Yokota J, Sakiyama T, Shibata T, Yamamoto M, Hirohashi S. 2008. Loss of Keap1 function activates Nrf2 and provides advantages for lung cancer cell growth. Cancer Res 68:1303–1309.

Roberts EC, Shapiro PS, Nahreini TS, Pages G, Pouyssegur J, Ahn NG. 2002. Distinct cell cycle timing requirements for extracellular signal-regulated kinase and phosphoinositide 3-kinase signaling pathways in somatic cell mitosis. Mol Cell Biol 22:7226–7241.

Rushworth SA, MacEwan DJ. 2011. The Role of Nrf2 and cytoprotection in regulating chemotherapy resistance of human leukemia cells. Cancers 3:1605–1621.

Sachdev D, Zhang X, Matise I, Gaillard-Kelly M, Yee D. 2010. The type I insulin-like growth factor receptor regulates cancer metastasis independently of primary tumor growth by promoting invasion and survival. Oncogene 29:251–262.

Sandusky GE, Mintze KS, Pratt SE, Dantzig AH. 2002. Expression of multidrug resistance-associated protein 2 (MRP2) in normal human tissues and carcinomas using tissue microarrays. Histopathology 41:65–74.

Singh A, Misra V, Thimmulappa RK, Lee H, Ames S, Hoque MO, Herman JG, Baylin SB, Sidransky D, Gabrielson E, Brock MV, Biswal S. 2006. Dysfunctional KEAP1–NRF2 interaction in non-small-cell lung cancer. PLoS Med 3:e420.

Stöckel B, König J, Nies AT, Cui Y, Brom M, Keppler D. 2000. Characterization of the 5′-flanking region of the human multidrug resistance protein 2 (MRP2) gene and its regulation in comparison withthe multidrug resistance protein 3 (MRP3) gene. Eur J Biochem 267:1347–1358.

Strömberg T, Ekman S, Girnita L, Dimberg LY, Larsson O, Axelson M, Lennartsson J, Hellman U, Carlson K, Österborg A, Vanderkerken K, Nilsson K, Jernberg-Wiklund H. 2006. IGF-1 receptor tyrosine kinase inhibition by the cyclolignan PPP induces G2/M-phase accumulation and apoptosis in multiple myeloma cells. Blood 107:669–678.

Sui H, Wang Y, Liu X, Zhou L, Yin P, Zhou S-F, Fan Z, Li Q. 2011. COX-2 contributes to P-glycoprotein-mediated multidrug resistance via phosphorylation of c-Jun at Ser63/73 in colorectal cancer. Carcinogenesis 32:667–675.

Tanno S, Tanno S, Mitsuuchi Y, Altomare DA, Xiao G-H, Testa JR. 2001. AKT activation up-regulates insulin-like growth factor I receptor expression and promotes invasiveness of human pancreatic cancer cells. Cancer Res 61:589–593.

Tarn C, Rink L, Merkel E, Flieder D, Pathak H, Koumbi D, Testa JR, Eisenberg B, von Mehren M, Godwin AK. 2008. Insulin-like growth factor 1 receptor is a potential therapeutic target for gastrointestinal stromal tumors. Proc Natl Acad Sci USA 105:8387–8392.

Thompson AD, Kakar SS. 2005. Insulin and IGF-1 regulate the expression of the pituitary tumor transforming gene (PTTG) in breast tumor cells. Febs Lett 579:3195–3200.

Whittaker S, Marais R, Zhu AX. 2010. The role of signaling pathways in the development and treatment of hepatocellular carcinoma. Oncogene 29: 4989–5005.

Xu W, Liu JW, Li CL, Wu HZ, Liu YW. 2008. Kaempferol-7-O-beta-D-glucoside (KG) isolated from *Smilax china* L. rhizome induces G(2)/M phase arrest and apoptosis on HeLa cells in a p53-independent manner. Cancer Lett 264:229–240.

Young LC, Campling BG, Cole SPC, Deeley RG, Gerlach JH. 2001. Multidrug resistance proteins MRP3, MRP1, and MRP2 in lung cancer. Clin Cancer Res 7:1798–1804.